Fatigue of bridges with a horizontal rotation axle under random wind load

Document Version:
Publisher's PDF, also known as Version of Record (includes final page, issue and volume numbers)

Please check the document version of this publication:

• A submitted manuscript is the version of the article upon submission and before peer-review. There can be important differences between the submitted version and the official published version of record. People interested in the research are advised to contact the author for the final version of the publication, or visit the DOI to the publisher's website.
• The final author version and the galley proof are versions of the publication after peer review.
• The final published version features the final layout of the paper including the volume, issue and page numbers.

[Link to publication](#)

Fatigue of bridges with a horizontal rotation axle under random wind load

J. Maljaars, R.D.J.M Steenbergen

TNO, the Netherlands

The operating mechanisms of movable bridges are subjected to various types of fluctuating loads which may induce fatigue damage. Wind load acting on the bridge deck – when the bridge is open – is one of the important load types. A wind load model is proposed that can be used in the fatigue design verification. The model is based on wind statistics. It is presented as a Markov matrix that gives the probability of the combinations of mean wind loads and wind load fluctuations. The model will be implemented in the new version of the standard NEN 6786.

Key words: Wind load, fatigue damage calculation, Markov matrix, hydraulic cylinder, gear tooth, axle, bascule bridge, movable bridge, drawbridge

1   Introduction

The operating mechanism of bascule bridges and other types of bridges with a horizontal rotating axle are subjected to various types of fluctuating loads, which may cause fatigue failure of parts of the mechanism. In order to check whether the fatigue life of the mechanism meets the design life, the engineer needs descriptions of the ranges and numbers of the load fluctuations during the design life. Fluctuating loads due to the motor and due to changes in pre-stress and self-weight action during opening and closing are a direct result of the design of the bridge, and can be determined by the engineer. Other types of fluctuating loads – predominantly system dynamics and wind loads – are often considered by approximate values. These approximate values generally result in overly conservative designs of the operating mechanism. In some special cases – e.g. in case of a bridge with a relatively long average opening period – it may even result in unsafe designs.

In the Dutch standard NEN 6786 the fluctuating wind load to be considered in fatigue verifications consists of a fixed portion of the static load for the ultimate limit state check.

The fluctuating wind load to be considered in the fatigue verification according to this standard can be written as:

$$\frac{F_{fat,d}}{\gamma_{s,fat,d}} = \frac{F_{s,\max,d} - F_{s,\min,d}}{\gamma_{s,d}} \psi_{fat} \qquad (1)$$

where

- $F_{fat,d}$ is the fluctuating wind load to be used in the fatigue checks
- $F_{s,\max,d}$ is the maximum load to be used in the ultimate limit state static checks
- $F_{s,\min,d}$ is the minimum load to be used in the ultimate limit state static checks
- $\gamma_{s,fat,d}$ is the partial factor for the fatigue load
- $\gamma_{s,d}$ is the partial factor for the ultimate limit state static load
- ψ_{fat} is the factor that relates the fluctuating wind load for fatigue to the wind load in the ultimate limit state reduction factor.

The stress resulting from the load $F_{fat,d}$ should be checked against the fatigue design strength of the considered part of the structure at 2 million cycles.

The value for the reduction factor ψ_{fat} is determined in Vrouwenvelder, Waarts and Van Staalduinen (1990) for the situation of a bridge with 500.000 openings during its life, where one opening consists of 2 minutes during which the bridge is being opened, 3 minutes during which the bridge is completely open, and 2 minutes during which the bridge is closed. The resulting value for ψ_{fat} = 0.25. This value is used in NEN 6786 for all bridges, independent of the number of openings and opening times. Although this check is easy to apply for the engineer, it does not account for the actual number of openings and the opening times per bridge. In addition, the maximum wind velocity at which the bridge is allowed to open varies per bridge. The ultimate limit state wind load is directly related to this maximum wind velocity. However, the fatigue wind load spectrum is less affected by the maximum wind velocity, because the number of cycles with high wind velocity is small. By specifying a fixed value for ψ_{fat} the standard ignores this effect.

This paper presents a wind load model to be used in the fatigue design check of the operating mechanism of bridges rotating around a horizontal axis, such as bascule bridges. The model is based on the principles of the Eurocode for wind actions on structures, EN 1991-1-4, in order to ensure consistency in the design. It provides a more accurate representation of the fluctuating wind load than the current method of Eq. (1), because it accounts for bridge-specific characteristics such as the maximum wind velocity, the

2

number of openings and the opening times. The wind load model can be used in combination with the other fluctuating load models.

2   Bridge response to wind actions.

The response of a structure subjected to wind action consists of background response and resonance. The background response is caused by wind load fluctuations taken by the structure. In case the lowest natural frequency of a structure, f_1, is sufficiently low, the structure may resonate due to the wind load. The resonance is negligible in case of high natural frequencies, because wind fluctuations with high frequencies have a low energy content. This is indicated in Figure 1. Figure 1a gives an example of the wind load, Figure 1b gives a schematic representation of a structure with a relatively high value of f_1 and Figure 1c gives a schematic representation of a structure with a relatively low value of f_1.
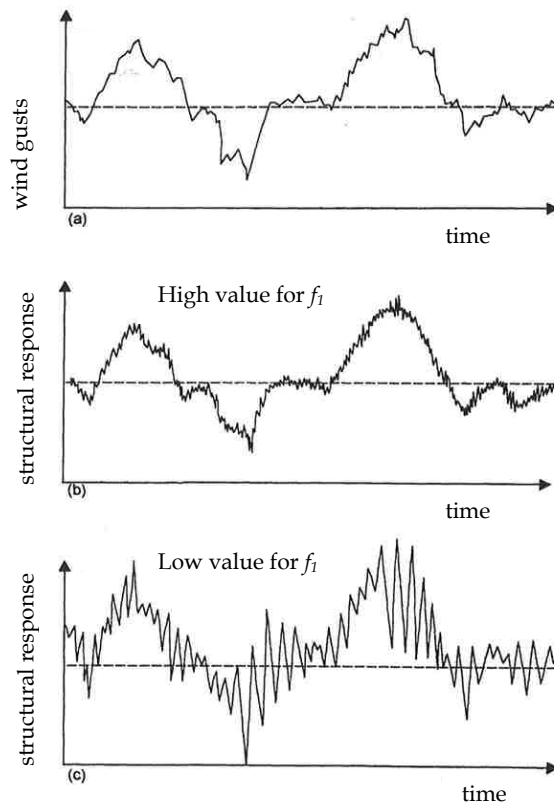

Figure 1: Response of a structure with a relatively high and a relatively low value for the lowest natural frequency, subjected to fluctuating wind loads (after Holmes, 2001)

The frequency of the wind gust that contain most energy, is around 0.05 Hz. For structures with f_1 larger than approximately 1 Hz, the exciting frequency is so low with respect to the natural frequency that the resonant dynamic response is negligible compared to the background response (after Holmes, 2001). Measurements on several types of bridge decks have indicated that f_1 is in the order of 1 to 3 Hz (Waarts and Van Staalduinen, 1990). Consequently, the bridge will not experience significant resonant dynamic response. Instead, the bridge deck will follow closely the time variation of the exciting forces. For this reason, the stress ranges relevant for the fatigue verification can directly be determined as a function of the wind velocity and the load frequency can be taken equal to the frequency of the wind gust fluctuations. The small effect of resonant dynamic response is accounted for by multiplying the quasi static response with a dynamic amplification factor, ϕ_w. For new bridges, a conservative value of the dynamic amplification ϕ_w = 1.15 is provided in NEN 6786.

3   Wind load and wind velocities

The wind velocity is divided into a component describing the 10 minutes mean wind velocity, $\overline{v}(t)$, and a component describing the fluctuations on this 10 minutes mean value, $\tilde{v}(t)$.

3.1   10-minutes mean wind velocity

The 10-minutes mean wind velocity $\overline{v}$ is usually expressed at a reference height of 10 m above ground level, $\overline{v}_{10}$. A Weibull distribution function is often considered for representing the probability density of $\overline{v}_{10}$ (Van Staalduinen, 1989):

$$f_v(\overline{v}_{10}) = \frac{k\,\overline{v}_{10}^{k-1}}{c^k}\exp(-\left(\frac{\overline{v}_{10}}{c}\right)^k) \tag{2}$$

As an example, Figure 2 provides $\overline{v}_{10}$ as based on measurements carried out by the KNMI at Schiphol, The Netherlands, in 1964. The figure also provides the Weibull distribution that fits the measurements.

Parameters c and k in Eq. (2) can be expressed as a function of the geographic location and the type of terrain. Considering the geographic location, the Dutch National Annex to EN 1991-1-4 divides The Netherlands in three wind areas. In each of the wind areas a choice
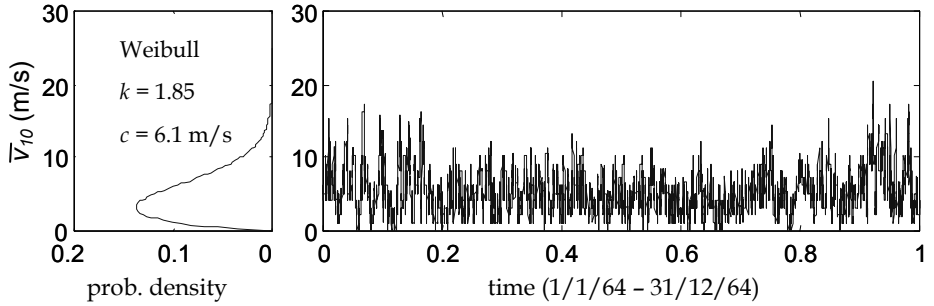
Figure 2: Weibull distribution of the 10-minute mean wind velocity as based on measurements at Schiphol in 1964

has to be made between three types of terrain. For bridges, two types of terrain are relevant:

- Terrain without buildings or terrain where buildings only cover a small part of the total area. The terrain roughness is set to $z_0 = 0.2$ m and the height with uniform wind velocity is set to $z_{min} = 4$ m for this type of terrain.
- Coastal area (or sea area). The terrain roughness is set to $z_0 = 0.005$ m and the height with uniform wind velocity is set to $z_{min} = 1$ m for this type of terrain.

The corresponding values for k and c in Eq. (2) are determined using the procedure in Van Staalduinen (1989) and are presented in Table 1.

The 10-minutes mean wind velocity at a certain height above ground level, $\overline{v}(z)$, can be determined with the following equations in EN 1991-1-4:

$$\overline{v}(z) = z_{cor}(z)\,\overline{v}_{10} \tag{3}$$

$$z_{cor}(z) = \begin{cases} \ln(\dfrac{z}{z_0}) / \ln(\dfrac{10\,\text{m}}{z_0}) & \text{for} \quad z \geq z_{min} \\[2mm] \ln(\dfrac{z_{min}}{z_0}) / \ln(\dfrac{10\,\text{m}}{z_0}) & \text{for} \quad z < z_{min} \end{cases} \tag{4}$$

Figure 3 presents the 10 minutes mean wind velocity for two of the terrain categories defined for The Netherlands, using Eq. (3) and (4). The figure indicates that the gradient in wind velocity over height is larger for built area than for coastal area.

Table 1: Weibull variables for the 10-min. mean wind velocity at reference height (10 m above ground level)

	non-densely built area (z_0 = 0.2 m, z_{min} = 4 m)		coastal area (z_0 = 0.005 m, z_{min} = 1 m)	
	k [-]	c [m/s]	k [-]	c [m/s]
Wind area I	1.85	6.1	1.85	7.9
Wind area II	1.85	5.5	1.85	7.1
Wind area III	1.75	4.9	1.75	6.4
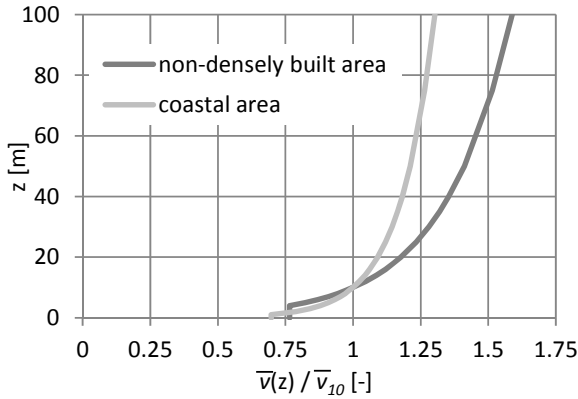
Figure 3: Relation between height above ground level and the normalised 10-minute mean wind velocity

simplified representation of this broad banded spectrum is obtained when assuming a narrow banded Gaussian process around the central frequency, f_c, Figure 4. The resulting narrow banded Gaussian process is schematically presented in Figure 5. Holmes (2001) and Wirsching and Light (1980) have shown that this narrow banded process is a conservative approximation for application to fatigue.

The ranges of the narrow banded Gaussian process, $\Delta\hat{v}$, are equal to two times the peak values, $\hat{v}$:

$$\Delta\hat{v} = 2\hat{v} \tag{5}$$

These peak values $\hat{v}$ can be described with a Rayleigh distribution function (Holmes, 2001):

$$f_{\hat{v}}(\hat{v}) = \frac{\hat{v}}{\sigma_v^2}\exp(-\frac{\hat{v}^2}{2\sigma_v^2}) \tag{6}$$

6
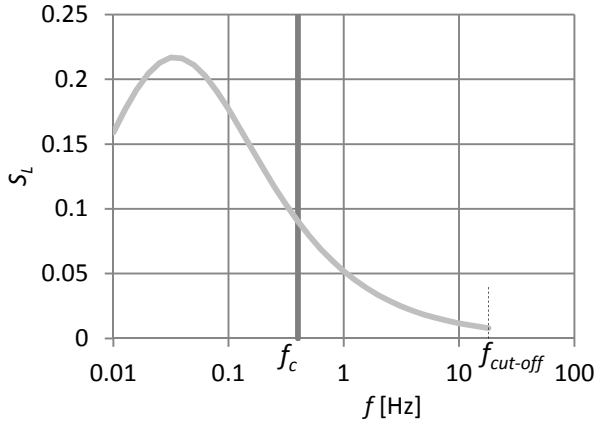
Figure 4: Spectral density S_L, describing the wind distribution as a function of the frequency f, for non-densely built area and $\overline{v}_{10}$ = 12 m/s
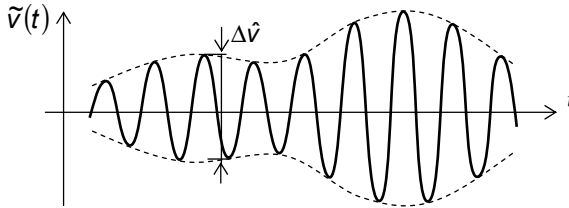
Figure 5: Wind fluctuations approximated by a narrow banded Gaussian process

where σ_v is the standard deviation of the Gaussian process. This standard deviation is related to the 10 minutes mean wind velocity via the turbulence intensity, I_v.

$$I_v(z) = \frac{\sigma_v}{\overline{v}(z)} \tag{7}$$

EN 1991-1-4 provides the following equation for the turbulence intensity:

$$I_v(z) = \begin{cases} \dfrac{1}{\ln(\dfrac{z}{z_0})} & \text{for} \quad z \geq z_{min} \\[4mm] \dfrac{1}{\ln(\dfrac{z_{min}}{z_0})} & \text{for} \quad z < z_{min} \end{cases} \tag{8}$$

From Eq. (3), (4), (7) and (8) it follows that σ_v is independent of the height above ground level. From Eq. (6) it subsequently follows that $\hat{v}$ is also independent of the height above ground level.

7

The frequency of the narrow banded Gaussian process is taken as the mean or central frequency of the wind spectrum, f_c. The central frequency of a power spectrum $P(f)$ is by definition equal to $f_c = \int\limits_0^\infty f \cdot P(f)df \Big/ \int\limits_0^\infty P(f)df$. In the case of the wind spectrum, the denominator is equal to σ_v^2 . Hence the central frequency of the wind spectrum is equal to:

$$f_c(z,f,\overline{v}) = \int\limits_0^{f_{\text{cut-off}}} \frac{f \cdot S_{vv}(z,f,\overline{v})}{\sigma_v^2} df = \int\limits_0^{f_{\text{cut-off}}} S_L(z,f,\overline{v}) df \qquad (9)$$

where

S_{vv} = variance spectrum.

S_L = non-dimensional power spectral density function, describing the wind distribution over frequencies.

f = frequency.

$f_{\text{cut-off}}$ = cut-off frequency.

The cut-off frequency is introduced because the integration in Eq. (9) to infinity results in f_c = infinity. The cut-off frequency should be selected in such a way that wind gusts with a frequency larger than the cut-off frequency have a negligible influence on the response of the bridge. Here, we apply $f_{\text{cut-off}} = 6 \times f_1$ because wind gusts with $f > 6\,f_1$ have very small energy content, and therefore do not result in stresses of any significance. Most bridges have a lowest natural frequency $f_1 \leq 3$ Hz (Section 2), so that we apply $f_{\text{cut-off}} = 18$ Hz. This is a conservative value. Wind gusts with a larger frequency do not result in stresses of any significance.

The non-dimensional power spectral density function, S_L in Eq. (9), can be written in terms of the reduced wind spectrum in EN 1991-1-4. The following equations are provided in that standard:

$$S_L(z,f,\overline{v}) = \frac{6.8\,f_L(z,f,\overline{v})}{\left(1+10.2\,f_L(z,f,\overline{v})\right)^{5/3}} \qquad (10)$$

$$f_L(z,f,\overline{v}) = \frac{f \cdot L(z)}{\overline{v}(z)} \qquad (11)$$

$$L(z) = \begin{cases} L_t \left(\dfrac{z}{z_t} \right)^{(0.67+0.05\, z_o)} & \text{for} \quad z \geq z_{\min} \\[4mm] L_t \left(\dfrac{z_{min}}{z_t} \right)^{(0.67+0.05\, z_o)} & \text{for} \quad z < z_{\min} \end{cases} \tag{12}$$

where

f_L = non-dimensional frequency.

S_L = non-dimensional power spectral density function, describing the wind distribution over frequencies.

L = turbulence length scale representing the average wind gust size.

L_t = 300 m.

z_t = 200 m.

The central frequency, f_c, is different for each value of the 10-minutes mean wind velocity, for each height (i.e. each opening angle) and for each bridge with its specific natural frequency and dimensions. Values for f_c for practical ranges of $\bar{v}_{10}$ and z have been determined using Eq. (9) to (12). The results are provided in Figure 6 for a bridge with f_1 = 3 Hz. This figure indicates that f_c increases with increasing 10-minutes mean wind velocity, and that the maximum value of f_c occurs for $z = 1$ and $z = 4$ m for coastal and non-densely built area, respectively.

It is difficult to determine f_1 in the design stage. Besides, the amount of work required by the engineer to determine f_c for each combination of $\bar{v}_{10}$ and z with Eq. (9) to (12) is so large, that this is unpractical. For this reason, a fixed value is adopted for f_c here, independent of the actual value of f_1, $\bar{v}_{10}$ and z. It is too conservative to apply the maximum value in Figure 6 for f_c, because the maximum wind velocity occurs only during a very short period in life, i.e. the majority of openings occur at a relatively low wind velocity. The value f_c = 0.4 Hz is adopted. This value is based on a number of simulations for various bridges, with the range of dimensions and wind regimes according to the cases in Section 6. For a bridge with a 1st natural frequency of 3 Hz in a non-densely built area and a span of 10 m, 20 m or 50 m, the fatigue life is underestimated by appr. 2 %, 8 % or 11 %, respectively, when adopting the fixed value f_c = 0.4 Hz. The underestimation is slightly larger for a bridge with a smaller 1st natural frequency or a bridge in a coastal area. Thus, the fixed value f_c = 0.4 Hz is safe for practical cases.
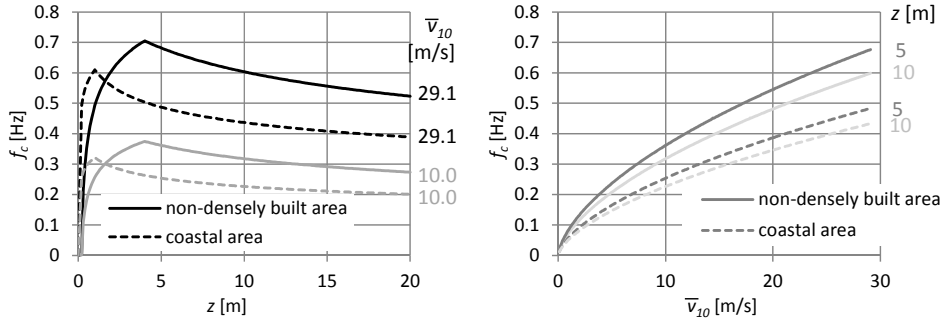
Figure 6: Central frequency as a function of z and $\overline{v}_{10}$, for $f_1 = 3$ Hz

3.2 Bridge opening regimes

Bascule bridges – as well as other bridges that can rotate around a horizontal axis – are operated up to a certain 10-minutes mean wind velocity at reference height, $\overline{v}_{10,max}$. The bridge is not opened when $\overline{v}_{10,max}$ is exceeded. This results in limiting the Weibull distribution of Eq. (2) to $\overline{v}_{10,max}$. Values for $\overline{v}_{10,max}$ are presented in Table 2. For reference, Table 2 also indicates the approximate number of annual days that the bridge cannot be operated when $\overline{v}_{10} > \overline{v}_{10,max}$.

Table 2: Maximum basic wind velocities $\overline{v}_{10,max}$ (m/s)

approximate average annual number of non-operating days	Wind area and terrain category					
	I-a [*]	I-b	II-a	II-b	III-a	III-b
4 times in 50 years	24.7	29.1	22.5	26.5	20.2	23.8
1/12	19.6	23.0	18.2	21.4	16.0	18.8
¼	18.1	21.3	16.7	19.7	14.5	17.0
½	17.3	20.3	15.8	18.6	13.4	15.8
1	16.3	19.2	14.8	17.4	12.5	14.7
2	15.3	18.0	13.7	16.1	11.6	13.7
3	14.7	17.3	13.2	15.5	11.0	12.9
7	13.3	15.6	11.8	13.9	9.9	11.7
14	12.2	14.4	10.7	12.6	8.8	10.4
28	10.9	12.8	9.4	11.1	7.7	9.1

[*] Terrain categories a = non-densely built area; b = coastal area

4 Derivation of the wind load model

4.1 Wind pressure on the bridge deck

NEN 6786 provides the relationship between the wind pressure, p, acting on the bridge deck and the wind load, q.

$$p = c_{\mathrm{dim}} c_t \, \phi_w \, q \tag{13}$$

where

c_{dim} = factor accounting for the bridge dimensions. For most bridges, $C_{\mathrm{dim}} \approx 0.95$.

c_t = wind shape factor (explained hereafter),

ϕ_w = dynamic amplification factor, equal to 1.15 (Section 2).

The wind load, q, is described by the dynamic pressure of incompressible fluid dynamics:

$$q = \tfrac{1}{2}\rho \, v^2 = \tfrac{1}{2}\rho(\bar{v} + \tilde{v})^2 = \tfrac{1}{2}\rho \, \bar{v}^2 + \rho \, \bar{v} \, \tilde{v} + \tfrac{1}{2}\rho \, \tilde{v}^2 \tag{14}$$

where ρ = density of air = 1.25 kg/m³. The last term in Eq. (14) is usually neglected. The approximate function then becomes:

$$q \approx \tfrac{1}{2}\rho \, \bar{v}^2 + \rho \, \bar{v} \, \tilde{v} \tag{15}$$

The wind shape factor, c_t, depends on the opening angle, α, of the bridge and the position of the bridge in relation to the wind direction. Values for c_t are experimentally derived in wind tunnel research, (Vrouwenvelder, Waarts, Van Staalduinen, 1990). The maximum values for c_t for all wind directions are provided in Figure 7. The values are derived in such a way that the wind load to be considered, q, is the wind load acting at the maximum height (top) of the bridge deck for the corresponding opening angle α.

4.2 Probability of $\bar{q}$ and Δq

The wind load of Eq. (15) is divided into a part related to the 10-min mean wind load, $\bar{q}$, and a part related to the wind fluctuation, $\tilde{q}$:

$$\bar{q} = \tfrac{1}{2}\rho \, \bar{v}^2 \tag{16}$$

$$\tilde{q} = \rho \, \bar{v} \, \tilde{v} \tag{17}$$

A Rayleigh distribution is used for the peaks of the wind fluctuations, Eq. (6). Consequently the peaks of the wind load, $\hat{q}$, are also described with a Rayleigh
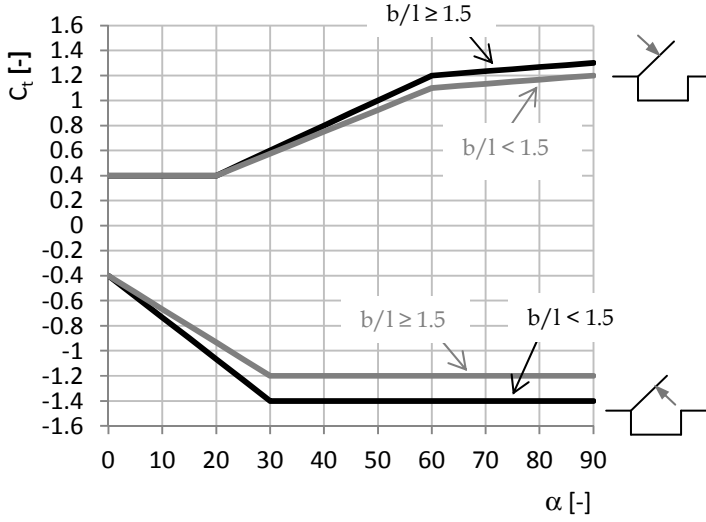
Figure 7: Wind shape factors (maximum values for all wind directions)

l = span of the bridge and b = width of the bridge, α = opening angle of the bridge

distribution:

$$f_q(\hat{q}) = \frac{\hat{q}}{\sigma_q^2} \exp(-\frac{\hat{q}^2}{2\sigma_q^2}) \tag{18}$$

Combining Eq. (7), (17) and (18) yields for $z = 10$ m:

$$f_q(\hat{q}_{10}) = \frac{\hat{q}_{10}}{I_v^2 \rho^2 \overline{v}_{10}^4} \exp(-\frac{\hat{q}_{10}^2}{2 I_v^2 \rho^2 \overline{v}_{10}^4}) \tag{19}$$

The Weibull distribution function for the 10 minutes mean wind velocity at height $z = 10$ m, $f_v(\overline{v}_{10})$, is provided with Eq.(2). The probability of a 10 minute mean wind velocity between $\overline{v}_{10}$ and $\overline{v}_{10} + d\overline{v}_{10}$ is:

$$P_1 = f_v(\overline{v}_{10})d\overline{v}_{10} \tag{20}$$

The conditional probability of a wind load peak due to the fluctuating part of the wind between $\hat{q}_{10}$ and $\hat{q}_{10} + d\hat{q}_{10}$, given a 10 minutes mean wind velocity is:

$$P_2 = f_q(\hat{q}_{10})d\hat{q}_{10} \tag{21}$$

Eq. (20) and (21) are combined to obtain the probability P of a 10 minutes mean wind velocity between $\overline{v}_{10}$ and $\overline{v}_{10} + d\overline{v}_{10}$ in combination with a wind peak between $\hat{q}_{10}$ and $\hat{q}_{10} + d\hat{q}_{10}$:

12

$$P = P_1 P_2 = f_v(\overline{v}_{10})\,d\overline{v}_{10}\,f_q(\hat{q}_{10})\,d\hat{q}_{10} \tag{22}$$

Note that this equation only holds under the approximation that the central frequency f_c is independent of $\overline{v}_{10}$, refer to Section 3.2. The 10 minutes average wind velocity and the peaks of the wind fluctuation are divided into blocks. The probability for each block with $\overline{v}_{10}$ between a and b and $\hat{q}_{10}$ between c and d, is equal to:

$$P_{b-a,d-c} = \int\limits_a^b\int\limits_c^d f_v(\overline{v}_{10}) f_q(\hat{q}_{10})\,d\hat{q}_{10}\,d\overline{v}_{10} \tag{23}$$

Substitution of Eq. (19) and (2) in Eq. (25) yields:

$$P_{b-a,d-c} = \int\limits_a^b\int\limits_c^d \frac{\hat{q}_{10}}{l_v^2\,\rho^2\,\overline{v}_{10}^4}\exp\left(-\frac{\hat{q}_{10}^2}{2\,l_v^2\,\rho^2\,\overline{v}_{10}^4}\right)\frac{k\,\overline{v}_{10}^{k-1}}{c^k}\exp\left(-\left(\frac{\overline{v}_{10}}{c}\right)^k\right)d\hat{q}_{10}\,d\overline{v}_{10} \tag{24}$$

Instead of $\overline{v}_{10}$ and $\hat{q}_{10}$, the wind load effects $\overline{q}_{10}$ and $\Delta\hat{q}_{10}$ are of interest for the fatigue calculation. The mean wind load effect $\overline{q}_{10}$ can be easily calculated with Eq. (16):

$$\overline{q}_{10} = \tfrac{1}{2}\rho\,\overline{v}_{10}^2 \tag{25}$$

The range is twice the peak value, see Figure 5:

$$\Delta\hat{q}_{10} = 2\,\hat{q}_{10} \tag{26}$$

4.3   *Markov matrix*

Eq. (26) is numerically solved for wind area, terrain categories and opening regimes of Table 2. The results are presented in so-called Markov matrices. Markov matrices are frequently applied in off-shore industry and usually indicate the number of stress cycles for each combination of average stress and stress range occurring during the life of the structure. In this paper, a slightly modified form is used, where each cell in a matrix indicates the probability of a certain value of $\overline{q}_{10}$ (on the horizontal axis) in combination with a certain value of $\Delta\hat{q}_{10}$ (on the vertical axis), Table 3. The probabilities have been calculated with Eq. (24)-(26). The resulting Markov matrices are indicated in Tables 4 to 9.

Table 3: Explanation of the Markov matrices of Tables 4-9

$\Delta\hat{q}_{10}$ $\overline{q}_{10}$	0 – 1 [N/m²]	1 – 2 [N/m²]	2 – 3 [N/m²]	…
0 – 1 [N/m²]	$P_{1-0,1-0}$	$P_{2-1,1-0}$	$P_{3-2,1-0}$	…
1 – 2 [N/m²]	$P_{1-0,2-1}$	$P_{2-1,2-1}$	$P_{3-2,2-1}$	…
…	…	…	…	…

The number of wind load cycles per matrix cell is obtained by multiplying the indicated probability $P(\overline{q}_{10}, \Delta\hat{q}_{10})$ in each cell of the matrix with the total number of wind load cycles, n_{tot}, during the life of the bridge:

$$n_{tot} = n_{op}\, T\, f_c \tag{27}$$

where

n_{op} = number of openings during the life of the bridge

T = average opening time

f_c = natural frequency = 0.4 Hz

Using Eq. (3), (13), (16), (17), (25) and (26), the wind pressures can be determined in correspondence with the wind loads:

$$\overline{p}(z) = \overline{q}_{10}\, z_{cor}^2\, c_{\dim}\, c_t(z)\, \phi_w \tag{28}$$

$$\Delta\hat{p}(z) = \Delta\hat{q}_{10}\, z_{cor}\, c_{\dim}\, c_t(z)\, \phi_w \tag{29}$$

The input for the fatigue calculation with respect to the wind pressure effects consists of the Markov matrix together with Eq. (27) to (29).

The opening regime of the bridge is considered by ignoring the columns of the Markov matrix with $\overline{v}_{10} > \overline{v}_{10,\max}$; the latter parameter according to Table 2. As a consequence, the sum of the probabilities in the remaining columns in the Markov matrix is no longer equal to unity. The probabilities in the remaining columns should therefore be multiplied with the correction factor $C_P = 1/\Sigma P$. This factor is approximately equal to the ratio 365 / (365-average annual no. of non-operating days) according to Table 2. However, C_P is close to unity for all opening regimes. This correction may therefore be ignored.

4.4   *Conservatisms*

The wind load model contains a number of conservatisms. The representation of the wind fluctuations with a narrow banded Gaussian process (Figure 5), the selection of the maximum wind shape factors for all wind directions (Figure 7), and the use of a fixed value for the central frequency, are conservative. In a follow up research, the conservatism should be quantified by comparing the resulting wind load model with actual measurements on bridges. In addition, this allows for deriving a partial factor for the fatigue wind load model, γ_{Ff}, corresponding with the target reliability. In this paper this partial factor is not further discussed.

14

Table 4: Markov matrix with probability P for wind area I, non-densely built area (z_0 = 0.2 m)

$\bar{q}_{10}$ [N/m²]	0-10	10-31	31-51	51-74	74-93	93-111	111-135	135-146	146-166	166-187	187-205	205-240	240-381	381-544
$\bar{v}_{10}$ [m/s]	0.0-4	4-7	7-9	9-10.9	10.9-12.2	12.2-13.3	13.3-14.7	14.7-15.3	15.3-16.3	16.3-17.3	17.3-18.1	18.1-19.6	19.6-24.7	24.7-29.5
$\Delta\hat{q}_{10}$ [N/m²]														
0-80	3.7E-1	3.6E-1	1.3E-1	4.3E-2	9.6E-3	3.3E-3	1.6E-3	2.9E-4	2.5E-4	1.0E-4	3.6E-5	2.4E-5	7.3E-6	0
80-160	0	1.6E-3	2.1E-2	2.9E-2	1.2E-2	5.5E-3	3.2E-3	6.4E-4	5.8E-4	2.5E-4	9.2E-5	6.4E-5	2.0E-5	8.8E-8
160-240	0	0	1.9E-4	3.0E-3	3.9E-3	2.9E-3	2.3E-3	5.8E-4	5.8E-4	2.8E-4	1.1E-4	8.3E-5	2.8E-5	1.4E-7
240-320	0	0	2.3E-7	9.4E-5	4.8E-4	7.4E-4	9.8E-4	3.3E-4	3.8E-4	2.2E-4	9.7E-5	7.9E-5	3.0E-5	1.7E-7
320-400	0	0	0	1.1E-6	2.7E-5	1.0E-4	2.6E-4	1.2E-4	1.8E-4	1.3E-4	6.6E-5	6.1E-5	2.7E-5	1.9E-7
400-480	0	0	0	0	7.4E-7	8.0E-6	4.5E-5	3.4E-5	6.5E-5	6.0E-5	3.6E-5	4.0E-5	2.2E-5	1.9E-7
480-560	0	0	0	0	0	3.8E-7	5.5E-6	6.5E-6	1.7E-5	2.2E-5	1.7E-5	2.2E-5	1.5E-5	1.8E-7
560-640	0	0	0	0	0	0	4.8E-7	9.3E-7	3.7E-6	6.5E-6	6.4E-6	1.1E-5	9.8E-6	1.6E-7
640-720	0	0	0	0	0	0	0	9.6E-8	6.0E-7	1.6E-6	2.0E-6	4.5E-6	5.8E-6	1.4E-7
720-800	0	0	0	0	0	0	0	0	7.7E-8	3.2E-7	5.6E-7	1.7E-6	3.2E-6	1.1E-7
800-880	0	0	0	0	0	0	0	0	0	5.3E-8	1.3E-7	5.4E-7	1.6E-6	8.6E-8
880-960	0	0	0	0	0	0	0	0	0	0	0	1.6E-7	7.8E-7	6.3E-8
960-1040	0	0	0	0	0	0	0	0	0	0	0	0	3.6E-7	0
1040-1120	0	0	0	0	0	0	0	0	0	0	0	0	1.6E-7	0

Table 5: Markov matrix with probability P for wind area I, coastal area (z_0 = 0.005 m)

$\bar{q}_{10}$ [N/m²]	0-10	10-31	31-63	63-102	102-130	130-152	152-187	187-203	203-230	230-258	258-284	284-331	331-529	529-544
$\bar{v}_{10}$ [m/s]	0.0-4	4-7	7-10	10-12.8	12.8-14.4	14.4-15.6	15.6-17.3	17.3-18	18-19.2	19.2-20.3	20.3-21.3	21.3-23	23-29.1	29.1-29.5
$\Delta\hat{q}_{10}$ [N/m²]														
0-70	2.5E-1	3.0E-1	2.3E-1	9.5E-2	1.9E-2	6.7E-3	4.2E-3	8.2E-4	7.8E-4	3.4E-4	1.5E-4	1.1E-4	4.5E-5	1.1E-7
70-140	0	1.3E-6	5.5E-3	3.0E-2	1.7E-2	8.7E-3	6.9E-3	1.6E-3	1.6E-3	7.6E-4	3.6E-4	2.7E-4	1.2E-4	3.0E-7
140-210	0	0	1.8E-6	9.0E-4	2.6E-3	2.7E-3	3.4E-3	1.1E-3	1.3E-3	7.1E-4	3.8E-4	3.0E-4	1.5E-4	4.5E-7
210-280	0	0	0	6.2E-6	1.1E-4	3.1E-4	3.4E-3	3.8E-4	5.9E-4	4.1E-4	2.6E-4	2.4E-4	1.4E-4	5.2E-7
280-350	0	0	0	0	1.7E-6	1.5E-5	1.0E-4	8.1E-5	1.7E-4	1.6E-4	1.3E-4	1.4E-4	1.1E-4	5.2E-7
350-420	0	0	0	0	0	3.5E-7	7.6E-6	1.1E-5	3.4E-5	4.7E-5	4.7E-5	6.9E-5	7.2E-5	4.7E-7
420-490	0	0	0	0	0	0	3.4E-7	8.6E-7	4.6E-6	9.7E-6	1.3E-5	2.7E-5	4.1E-5	3.9E-7
490-560	0	0	0	0	0	0	0	0	4.3E-7	1.5E-6	3.0E-6	8.4E-6	2.1E-5	2.9E-7
560-630	0	0	0	0	0	0	0	0	0	1.7E-7	5.1E-7	2.2E-6	9.6E-6	2.0E-7
630-700	0	0	0	0	0	0	0	0	0	0	7.0E-8	4.8E-7	4.1E-6	1.3E-7
700-770	0	0	0	0	0	0	0	0	0	0	0	8.8E-8	1.7E-6	7.8E-8
770-840	0	0	0	0	0	0	0	0	0	0	0	0	6.4E-7	0
840-910	0	0	0	0	0	0	0	0	0	0	0	0	2.4E-7	0
910-980	0	0	0	0	0	0	0	0	0	0	0	0	8.5E-8	0

Table 6: Markov matrix with probability P for wind area II, non-densely built area (z_0 = 0.2 m)

$\bar{q}_{10}$ [N/m²]	0-10	10-23	23-40	40-55	55-72	72-87	87-109	109-117	117-123	123-156	156-174	174-207	207-316	316-456
$\bar{v}_{10}$ [m/s]	0.0-4	4-6	6-8	8-9.4	9.4-10.7	10.7-11.8	11.8-13.2	13.2-13.7	13.7-14	14-15.8	15.8-16.7	16.7-18.2	18.2-22.5	22.5-27
$\Delta\hat{q}_{10}$ [N/m²]														
0-70	4.2E-1	2.7E-1	1.6E-1	4.5E-2	1.6E-2	5.1E-3	2.3E-3	3.3E-4	1.3E-4	3.3E-4	3.9E-5	2.0E-5	4.6E-6	0
70-140	0	3.0E-4	1.5E-2	2.2E-2	1.6E-2	7.4E-3	4.2E-3	6.8E-4	2.9E-4	7.6E-4	9.8E-5	5.2E-5	1.3E-5	7.6E-8
140-210	0	0	5.6E-5	1.1E-3	3.0E-3	3.0E-3	2.6E-3	5.6E-4	2.6E-4	7.6E-4	1.2E-4	6.6E-5	1.8E-5	1.2E-7
210-280	0	0	0	1.2E-5	1.9E-4	5.0E-4	8.6E-4	2.7E-4	1.4E-4	5.0E-4	9.7E-5	6.2E-5	1.9E-5	1.4E-7
280-350	0	0	0	0	4.6E-6	4.1E-5	1.7E-4	8.3E-5	5.0E-5	2.4E-4	6.2E-5	4.6E-5	1.7E-5	1.6E-7
350-420	0	0	0	0	0	1.8E-6	2.1E-5	1.7E-5	1.3E-5	8.5E-5	3.2E-5	2.9E-5	1.3E-5	1.6E-7
420-490	0	0	0	0	0	0	1.7E-6	2.4E-6	2.2E-6	2.4E-5	1.4E-5	1.6E-5	9.1E-6	1.4E-7
490-560	0	0	0	0	0	0	9.9E-8	2.3E-7	2.8E-7	5.5E-6	4.8E-6	7.3E-6	5.7E-6	1.3E-7
560-630	0	0	0	0	0	0	0	0	0	1.0E-6	1.4E-6	2.9E-6	3.3E-6	1.0E-7
630-700	0	0	0	0	0	0	0	0	0	1.6E-7	3.5E-7	1.0E-6	1.7E-6	8.0E-8
700-770	0	0	0	0	0	0	0	0	0	0	7.2E-8	3.2E-7	8.5E-7	5.9E-8
770-840	0	0	0	0	0	0	0	0	0	0	0	8.8E-8	4.0E-7	0
840-910	0	0	0	0	0	0	0	0	0	0	0	0	1.8E-7	0
910-980	0	0	0	0	0	0	0	0	0	0	0	0	7.5E-8	0

Table 7: *Markov matrix with probability P for wind area II, coastal area (z_0 = 0.005 m)*

$\bar{q}_{10}$ [N/m²]	0-10	10-31	31-51	51-77	77-99	99-121	121-150	150-162	162-189	189-216	216-243	243-286	286-439	439-456
$\bar{v}_{10}$ [m/s]	0.0-4	4-7	7-9	9-11.1	11.1-12.6	12.6-13.9	13.9-15.5	15.5-16.1	16.1-17.4	17.4-18.6	18.6-19.7	19.7-21.4	21.4-26.5	26.5-27
$\Delta\hat{q}_{10}$ [N/m²]														
0-60	2.9E-1	3.3E-1	1.6E-1	9.0E-2	2.7E-2	1.0E-2	5.2E-3	9.0E-4	1.0E-3	3.9E-4	1.5E-4	8.3E-5	2.7E-5	1.2E-7
60-120	0	2.1E-5	3.8E-3	2.0E-2	1.8E-2	1.1E-2	7.7E-3	1.6E-3	2.0E-3	8.5E-4	3.5E-4	2.0E-4	7.2E-5	3.2E-7
120-180	0	0	5.5E-7	2.8E-4	1.6E-3	2.6E-3	3.3E-3	9.7E-4	1.5E-3	7.6E-4	3.6E-4	2.3E-4	9.3E-5	4.7E-7
180-240	0	0	0	5.4E-7	3.1E-5	1.9E-4	6.0E-4	2.9E-4	6.0E-4	4.1E-4	2.4E-4	1.8E-4	8.8E-5	5.5E-7
240-300	0	0	0	0	1.8E-7	5.4E-6	5.6E-5	4.8E-5	1.5E-4	1.5E-4	1.2E-4	1.1E-4	6.8E-5	5.4E-7
300-360	0	0	0	0	0	6.5E-8	2.9E-6	4.6E-6	2.4E-5	4.0E-5	4.2E-5	5.3E-5	4.5E-5	4.8E-7
360-420	0	0	0	0	0	0	8.6E-8	2.6E-7	2.6E-6	7.5E-6	1.2E-5	2.1E-5	2.6E-5	3.8E-7
420-480	0	0	0	0	0	0	0	0	1.9E-7	1.0E-6	2.5E-6	6.6E-6	1.3E-5	2.8E-7
480-540	0	0	0	0	0	0	0	0	0	1.1E-7	4.2E-7	1.7E-6	5.9E-6	1.9E-7
540-600	0	0	0	0	0	0	0	0	0	0	5.5E-8	3.8E-7	2.5E-6	1.2E-7
600-660	0	0	0	0	0	0	0	0	0	0	0	7.2E-8	9.7E-7	6.8E-8
660-720	0	0	0	0	0	0	0	0	0	0	0	0	3.6E-7	0
720-780	0	0	0	0	0	0	0	0	0	0	0	0	1.3E-7	0
780-840	0	0	0	0	0	0	0	0	0	0	0	0	4.3E-8	0

Table 8: *Markov matrix with probability P for wind area III, non-densely built area (z_0 = 0.2 m)*

$\bar{q}_{10}$ [N/m²]	0-6	6-19	19-31	31-37	37-48	48-61	61-76	76-84	84-98	98-112	112-131	131-160	160-255	255-375
$\bar{v}_{10}$ [m/s]	0.0-3	3-5.5	5.5-7	7-7.7	7.7-8.8	8.8-9.9	9.9-11	11-11.6	11.6-12.5	12.5-13.4	13.4-14.5	14.5-16	16-20.2	20.2-24.5
$\Delta\hat{q}_{10}$ [N/m²]														
0-60	3.4E-1	3.6E-1	1.3E-1	3.5E-2	3.0E-2	1.3E-2	5.2E-3	1.3E-3	9.8E-4	4.2E-4	1.9E-4	7.4E-5	1.8E-5	1.5E-7
60-120	0	2.3E-4	8.3E-3	9.6E-3	1.7E-2	1.3E-2	7.5E-3	2.3E-3	1.9E-3	9.1E-4	4.6E-4	1.9E-4	5.0E-5	4.2E-7
120-180	0	0	1.0E-5	1.2E-4	1.1E-3	2.6E-3	3.0E-3	1.3E-3	1.4E-3	8.2E-4	4.8E-4	2.2E-4	6.6E-5	6.4E-7
180-240	0	0	0	1.1E-7	1.5E-5	1.7E-4	5.3E-4	4.0E-4	5.8E-4	4.5E-4	3.3E-4	1.9E-4	6.7E-5	7.8E-7
240-300	0	0	0	0	0	4.2E-6	4.5E-5	6.5E-5	1.5E-4	1.7E-4	1.7E-4	1.2E-4	5.6E-5	8.3E-7
300-360	0	0	0	0	0	0	2.1E-6	6.1E-6	2.5E-5	4.5E-5	6.5E-5	6.6E-5	4.0E-5	8.1E-7
360-420	0	0	0	0	0	0	5.4E-8	3.4E-7	2.7E-6	8.6E-6	1.9E-5	2.9E-5	2.6E-5	7.3E-7
420-480	0	0	0	0	0	0	0	0	2.1E-7	1.2E-6	4.6E-6	1.1E-5	1.5E-5	6.2E-7
480-540	0	0	0	0	0	0	0	0	0	1.3E-7	8.8E-7	3.4E-6	7.6E-6	4.9E-7
540-600	0	0	0	0	0	0	0	0	0	0	1.4E-7	9.2E-7	3.7E-6	3.7E-7
600-660	0	0	0	0	0	0	0	0	0	0	0	2.2E-7	1.7E-6	2.6E-7
660-720	0	0	0	0	0	0	0	0	0	0	0	0	7.1E-7	1.8E-7
720-780	0	0	0	0	0	0	0	0	0	0	0	0	3.0E-7	1.2E-7
780-840	0	0	0	0	0	0	0	0	0	0	0	0	1.2E-7	7.2E-8

Table 9: *Markov matrix with probability P for wind area III, coastal area (z_0 = 0.005 m)*

$\bar{q}_{10}$ [N/m²]	0-8	8-23	23-40	40-52	52-68	68-86	86-104	104-117	117-135	135-156	156-181	181-221	221-354	354-375
$\bar{v}_{10}$ [m/s]	0.0-3.5	3.5-6	6-8	8-9.1	9.1-10.4	10.4-11.7	11.7-12.9	12.9-13.7	13.7-14.7	14.7-15.8	15.8-17	17-18.8	18.8-23.8	23.8-24.5
$\Delta\hat{q}_{10}$ [N/m²]														
0-50	2.9E-1	3.0E-1	1.8E-1	6.3E-2	4.4E-2	2.2E-2	9.4E-3	3.2E-3	2.2E-3	1.2E-3	5.6E-4	2.9E-4	9.2E-5	6.4E-7
50-100	0	2.2E-6	2.5E-3	8.1E-3	1.6E-2	1.6E-2	1.1E-2	4.8E-3	3.8E-3	2.3E-3	1.2E-3	6.9E-4	2.4E-4	1.8E-6
100-150	0	0	1.5E-7	2.0E-5	4.1E-4	1.8E-3	2.8E-3	2.0E-3	2.1E-3	1.7E-3	1.1E-3	7.2E-4	3.0E-4	2.6E-6
150-200	0	0	0	1.5E-6	4.6E-5	2.5E-4	3.4E-4	5.8E-4	6.7E-4	5.9E-4	5.1E-4	2.7E-4	3.0E-6	
200-250	0	0	0	0	3.6E-7	8.8E-6	2.8E-5	8.6E-5	1.7E-4	2.2E-4	2.6E-4	2.0E-4	2.9E-6	
250-300	0	0	0	0	0	1.4E-7	1.1E-6	7.4E-6	2.6E-5	5.6E-5	1.0E-4	1.2E-4	2.6E-6	
300-350	0	0	0	0	0	0	3.7E-7	2.8E-6	1.0E-5	3.3E-5	6.4E-5	2.0E-6		
350-400	0	0	0	0	0	0	0	2.0E-7	1.4E-6	8.2E-6	3.0E-5	1.4E-6		
400-450	0	0	0	0	0	0	0	0	1.5E-7	1.7E-6	1.3E-5	9.5E-7		
450-500	0	0	0	0	0	0	0	0	0	2.9E-7	5.2E-6	5.8E-7		
500-550	0	0	0	0	0	0	0	0	0	0	2.0E-6	3.2E-7		
550-600	0	0	0	0	0	0	0	0	0	0	7.2E-7	1.7E-7		
600-650	0	0	0	0	0	0	0	0	0	0	2.5E-7	8.1E-8		
650-700	0	0	0	0	0	0	0	0	0	0	8.3E-8	0		

5 Application of the wind load model in fatigue damage calculations

5.1 Concept of fatigue damage

The fatigue strength is usually described by an S-N curve:

$$N \, \Delta \hat{s}^m = K \tag{30}$$

where N is the number of cycles at failure as determined in fatigue tests, and m and K are parameters depending on the type of structural detail. Values for m and K are provided in standards such as ISO 6336-3, and are based on tests. In general, m and K depend on the mean stress $\bar{s}$ and on the stress fluctuation $\Delta \hat{s}$.

In case of a constant amplitude load, the fatigue damage D is defined as the ratio between the number of cycles occurring during the life, n, and the number of cycles to failure, N. Thus, $D = 0$ indicates that there is no fatigue damage and $D = 1$ indicates failure. In case of a variable amplitude load, consisting of k different stress ranges and corresponding no. of cycles, the fatigue damage is usually expressed by the Palmgren-Miner linear damage hypothesis according to Palmgren (1924) and Miner (1945):

$$D = \sum_{i=1}^{k} \frac{n_i}{N_i} \tag{31}$$

where

n_i = number of cycles during the life with mean stress $\bar{s}_i$ and stress fluctuation $\Delta \hat{s}_i$.

N_i = number of cycles to failure for mean stress $\bar{s}_i$ and stress fluctuation $\Delta \hat{s}_i$, determined with Eq. (30).

5.2 Elaboration for a non-rotating part of the bridge opening mechanism

This section gives an example of the fatigue damage calculation for fixed parts of the bridge opening mechanism. An example of such a part is a hydraulic cylinder. The stress cycles induced by wind loading during one opening are schematically indicated in Figure 8. In high cycle fatigue, linear elastic material behaviour is to be assumed. Hence, a linear relationship exists between the stress due to wind, s_w, and the wind pressure, p: $s = C \cdot p$, where C is the ratio between the stress in the considered part and the wind pressure on the bridge. This parameter, which is calculated by the engineer, is different for each part of a bridge and usually depends on the opening angle. For each opening angle α and for each
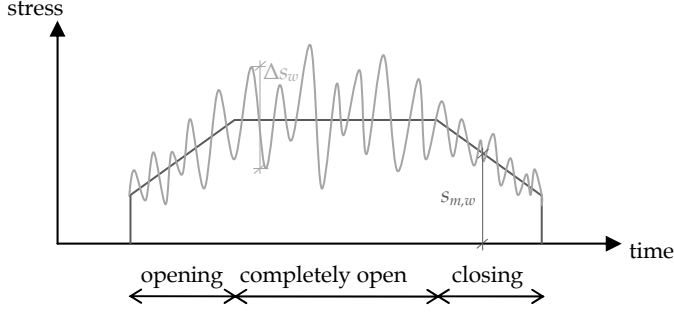
Figure 8: Stress cycles induced by wind loading on a fixed part during one bridge opening

cell in the Markov Matrix, the stress range and the mean stress can now be determined using Eq. (28) and (29):

$$\Delta \hat{s}_w(\alpha, \Delta \hat{q}_{10}) = \left| C(\alpha) \Delta \hat{q}_{10} \, z_{cor}(\alpha) c_{\dim} c_t(\alpha) \phi_w \right| \tag{32}$$

$$\overline{s}_w(\alpha, \overline{q}_{10}) = C(\alpha) \overline{q}_{10} \, z_{cor}^2(\alpha) c_{\dim} c_t(\alpha) \phi_w \tag{33}$$

If the structural part is also loaded by the self-weight of the bridge deck, s_{weight}, the average stress value is equal to:

$$\overline{s}(\alpha, \overline{q}_{10}) = \overline{s}_w(\alpha, \overline{q}_{10}) + s_{\text{weight}}(\alpha) \tag{34}$$

The values for $\overline{q}_{10}$ and $\Delta \hat{q}_{10}$ in Eq. (32) and (33) are indicated on the horizontal and vertical axes, respectively, of the Markov matrix. These values must be selected for each cell of the Markov matrix. The corresponding number of cycles for that cell is obtained by multiplying the probability in the cell with the total number of cycles of Eq. (27):

$$n_w(\alpha, \overline{q}_{10}, \Delta \hat{q}_{10}) = P(\overline{q}_{10}, \Delta \hat{q}_{10}) n_{op} \, T(\alpha) f_c \tag{35}$$

Where $P(\overline{q}_{10}, \Delta \hat{q}_{10})$ is the probability indicated in the cell of the Markov matrix, f_c is the central frequency taken as 0.4 Hz, n_{op} is the total number of openings during the life of the bridge and T is the time at opening angle α.

The fatigue damage is determined for each cell of the Markov matrix using Eq. (30) - (32), (34) and (35):

$$D_w(\alpha, \overline{q}_{10}, \Delta \hat{q}_{10}) = \frac{n_w(\alpha, \overline{q}_{10}, \Delta \hat{q}_{10}) \left[\Delta \hat{s}_w(\alpha, \Delta \hat{q}_{10}) \right]^m}{K} \tag{36}$$

Because m and K depend on $\bar{s}_w$ and $\Delta\hat{s}_w$, m and K are different for each cell of the Markov matrix.

Using the Palmgren-Miner linear damage hypothesis, the total fatigue damage due to wind actions, $D_{w,tot}$, is equal to the sum of the damages determined for each cell of the Markov matrix:

$$D_{w,\text{tot}} = \sum D_w(\alpha, \bar{q}_{10}, \Delta\hat{q}_{10}) \tag{37}$$

The value of $D_{w,tot}$ should be smaller than unity. As a conservative approach, the calculation can be carried out twice, for wind acting in the two opposite directions in Figure 7, and $D_{w,tot}$ should be smaller than unity for both cases.

The calculation provided here considers wind action only. However, other types of loading act simultaneously. This is schematically indicated in Figure 9, where s_T is the stress due to restrained thermal expansion and s_{pre} is the pre-stress. A rainflow analysis of this stress process results in:

–   The stress cycles for the wind fluctuations Δs_w, described by Eq. (32) to (35);
–   The maximum stress cycle Δs_1, with one cycle per opening;
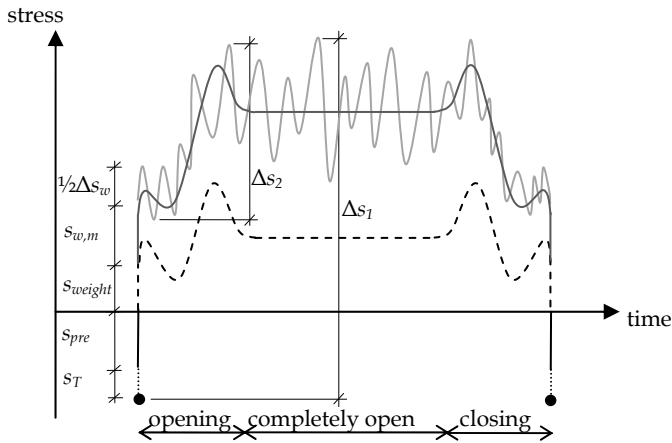–   The one-but-maximum stress cycles Δs_2, with two half cycles per opening.

Figure 9: Stress cycles in a fixed part during one bridge opening

Although the frequency of stress cycles Δs_1 and Δs_2 is much lower than that of Δs_w, the contribution of Δs_1 and Δs_2 to the fatigue damage can be significant for structural parts with an S-N curve having a large value of m (Eq. 30). The maximum wind fluctuation during an opening is relevant for Δs_1 and Δs_2. It is possible to derive Markov matrices for the maximum wind fluctuations during openings. However, this complicates the calculation for the engineer in practice. For this reason we use an approximate value for the contribution of the wind to Δs_1 and Δs_2:

$$s_{w,\max}(\alpha, q_{m,10}) = \overline{s}_w(\alpha, q_{m,10}) + \overline{s}_w(\alpha, q_{m,10}) \frac{7}{\ln \dfrac{z(\alpha)}{z_0}} \tag{38}$$

The last part of Eq. (38) represents the expectation of the maximum wind fluctuation, and is in agreement with the wind load for the static design check in EN 1991-1-4. The value of $\overline{s}_w(\alpha, q_{m,10})$ can be determined with Eq. (33). The contribution of the wind load according to Eq. (38) should be added to the other stress components indicated in Figure 9, and should be evaluated for all opening angles α. The maximum total stress range of all opening angles should be selected for Δs_1 and Δs_2.

5.3   *Elaboration for a rotating part of the bridge opening mechanism*

This section gives an example of the fatigue damage calculation for rotating parts of the bridge opening mechanism. The stress cycles may either be jump stress cycles, or fully reversed stress cycles. Examples of such parts are gear teeth or axles, respectively. The stress cycles induced by wind loading during one opening for a gear tooth are schematically indicated in Figure 10. For simplicity, in this figure it is assumed that the gear tooth is loaded by wind load only. During opening and closing, the gear is rotating while it is fixed during complete opening. Depending on the position of the considered
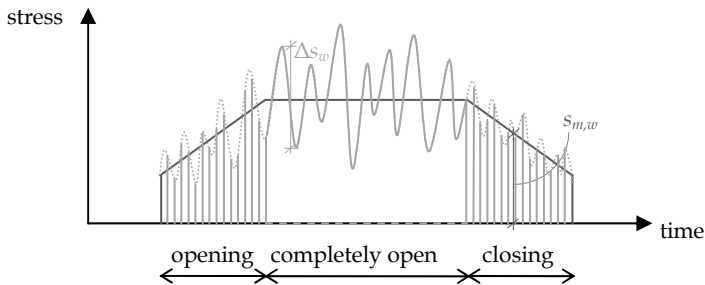

Figure 10: Stress cycles induced by wind loading on a rotating part during one bridge opening

tooth, it may or may not be loaded during complete opening. We assume that the rotating frequency of the gear, f_ω, is larger than the central frequency of the wind spectrum, f_c.

The stress cycles during complete opening are identical to those for a fixed part, Eq. (32)-(35). The stress cycles during opening and closing are approximated with:

-   25 % stress cycles coinciding with the peaks of the wind fluctuations: Δs_a.
-   25 % stress cycles coinciding with the valleys of the wind fluctuations: Δs_b.
-   50 % stress cycles exactly in between the peaks and valleys: Δs_c.

For each opening angle α and for each cell in the Markov matrix, the stress ranges are determined as:

$$\Delta s_a(\alpha, q_{m,10}, \Delta q_{10}) = C(\alpha) q_{m,10} z_{cor}^2(\alpha) c_{\dim} c_t(\alpha) \phi_w + \left| \frac{1}{2} C(\alpha) \Delta q_{10} z_{cor}(\alpha) c_{\dim} c_t(\alpha) \phi_w \right| \qquad (39)$$

$$\Delta s_b(\alpha, q_{m,10}, \Delta q_{10}) = C(\alpha) q_{m,10} z_{cor}^2(\alpha) c_{\dim} c_t(\alpha) \phi_w - \left| \frac{1}{2} C(\alpha) \Delta q_{10} z_{cor}(\alpha) c_{\dim} c_t(\alpha) \phi_w \right| \qquad (40)$$

$$\Delta s_c(\alpha, q_{m,10}, \Delta q_{10}) = C(\alpha) q_{m,10} z_{cor}^2(\alpha) c_{\dim} c_t(\alpha) \phi_w \qquad (41)$$

If the structural part is also loaded by the self-weight of the bridge deck, the corresponding stress s_{weight} should be added to Eq. (39)-(41). The mean stress level per cycle is half the stress range. The numbers of cycles are:

$$n_a(\alpha, q_{m,10}, \Delta q_{10}) = 0.25\, P(q_{m,10}, \Delta q_{10})\, n_{op}\, T(\alpha)\, f_\omega \qquad (42)$$

$$n_b(\alpha, q_{m,10}, \Delta q_{10}) = 0.25\, P(q_{m,10}, \Delta q_{10})\, n_{op}\, T(\alpha)\, f_\omega \qquad (43)$$

$$n_c(\alpha, q_{m,10}, \Delta q_{10}) = 0.50\, P(q_{m,10}, \Delta q_{10})\, n_{op}\, T(\alpha)\, f_\omega \qquad (44)$$

The same remarks and solution apply regarding the maximum stress range per opening, Δs_1.

6 Calculation examples

6.1 Example of a non-rotating part

Consider a hydraulic cylinder in a bridge with a number of openings during the life of n_{op} = 500000 and a maximum height (at full opening) l = 20 m and a width of b = 10 m. The bridge is situated in wind area II, non-densely built, so that Table 6 applies. Each opening consists of 2 minutes during which the bridge is being opened, 3 minutes during which the bridge is completely open, and 2 minutes during which the bridge is closed. The stress due to self-weight is $s_{weight}(\alpha) = 15$ N/mm² $\cdot \cos(\alpha)$. The value of parameter C, describing the relationship between wind pressure and stress, depends on the geometry of the structure. In the example, the ratio between the stress in the cylinder and the wind pressure on the bridge is taken as $C = 1.8.10^5$ [-] independently of the opening angle. The bridge is operated up to a maximum 10-minutes wind velocity at reference height of $\overline{v}_{10,max}$ = 14 m/s. The design values of the ultimate tensile strength and the fatigue strength at $2 \cdot 10^6$ cycles of the part under consideration is f_{td} = 519 N/mm² and $f_{fat,re,d}$= 37 N/mm². The standard NEN 6786 provides the S-N curve according to Figure 11 (fully reversed stress condition). The S-N curve is described with Eq. (45) to (48) (for fully and for non-reversed stress conditions):
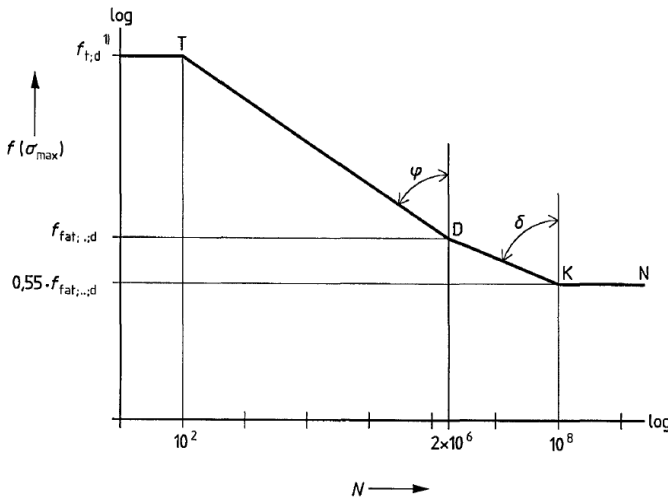

Figure 11: S-N curve according to NEN 6786 for fully reversed stress condition ($\overline{s}$ = 0) on the basis of the stress peak, σ_{max}

$$N \, \Delta \hat{s}^m = K \tag{45}$$

$$m = \begin{cases} \dfrac{\log 2 \cdot 10^6 - \log 10^2}{\log f_{td} - \log f_{fat,re,d}} & \text{for} \quad \Delta \hat{s} > 2 f_{fat,re,d}(1 - \dfrac{|\bar{s}|}{f_{td}}) \\[4mm] \dfrac{\log 2 \cdot 10^6 - \log 10^2}{\log f_{td} - \log f_{fat,re,d}} + 2 & \text{for} \quad \Delta \hat{s} \le 2 f_{fat,re,d}(1 - \dfrac{|\bar{s}|}{f_{td}}) \end{cases} \tag{46}$$

$$K = \begin{cases} 0 & \text{if} \quad \Delta \hat{s} > 2 f_{td}(1 - \dfrac{|\bar{s}|}{f_{td}}) \\[3mm] K_1 & \text{if} \quad 0.55 \times 2 f_{fat,re,d}(1 - \dfrac{|\bar{s}|}{f_{td}}) < \Delta \hat{s} \le 2 f_{td}(1 - \dfrac{|\bar{s}|}{f_{td}}) \\[3mm] \infty & \text{if} \quad \Delta \hat{s} < 0.55 \times 2 f_{fat,re,d}(1 - \dfrac{|\bar{s}|}{f_{td}}) \end{cases} \tag{47}$$

$$K_1 = 2 \cdot 10^6 \left(2 f_{fat,re,d}(1 - \dfrac{|\bar{s}|}{f_{td}}) \right)^{m_d} \tag{48}$$

For each opening angle α and for each cell in the Markov Matrix of Table 6, the stress range, the mean stress and the number of cycles are determined with Eq. (4) and (32) to (35) and with the parameters in Table 1 ($z_0 = 0.2$ m, $z_{min} = 4$ m). As an example, for the boxed cell in Table 6 with 117 N/m² $\le \bar{q}_{10} < 123$ N/m² and 490 N/m² $\le \Delta\hat{q}_{10} < 560$ N/m², and for an opening angle $\alpha = 90$ °:

$$z_{cor} = \frac{\ln \dfrac{l \cos \alpha}{z_0}}{\ln \dfrac{10\,\text{m}}{z_0}} = \frac{\ln \dfrac{20\,\text{m}}{0.2\,\text{m}}}{\ln \dfrac{10\,\text{m}}{0.2\,\text{m}}} = 1.18 \tag{49}$$

$$\begin{aligned} \Delta \hat{s}_w &= \left| C \, \Delta\hat{q}_{10} \, z_{cor} \, c_{\dim} \, c_t \, \phi_w \right| \\ &= 1.8 \cdot 10^5 \times 560 \; \text{N}\big/\text{m}^2 \times 1.18 \times 0.95 \times 1.3 \times 1.15 = 168 \; \text{N}\big/\text{mm}^2 \end{aligned} \tag{50}$$

$$\begin{aligned} \bar{s}_w &= C \, \bar{q}_{10} \, z_{cor}^2 \, c_{\dim} \, c_t \, \phi_w \\ &= 1.8 \cdot 10^5 \times 123 \; \text{N}\big/\text{m}^2 \times 1.18^2 \times 0.95 \times 1.3 \times 1.15 = 43 \; \text{N}\big/\text{mm}^2 \end{aligned} \tag{51}$$

$$\bar{s} = \bar{s}_w + s_{\text{weight}} = 43 \; \text{N}\big/\text{mm}^2 + 15 \; \text{N}\big/\text{mm}^2 \cos 90° = 43 \; \text{N}\big/\text{mm}^2 \tag{52}$$

$$n_w = P(\bar{q}_{10}, \Delta\hat{q}_{10}) \, n_{op} \, T \, f_c = 2.8 \cdot 10^{-7} \times 500000 \times 180 \; \text{s} \times 0.4 \; \text{Hz} = 10 \tag{53}$$

For this combination of $\Delta \hat{s}_w$ and $\bar{s}_w$, the parameters m and K of the S-N curve are equal to (Eq. (45)-(48)): $m = 3.75$ and $K = 1.5 \cdot 10^{13}$ [N/mm²]^m. The contribution to the fatigue damage is calculated using Eq. (36):

$$D_w = \frac{n_w \Delta \hat{s}_w^m}{K} = \frac{10(168 \text{ N}/\text{mm}^2)^{3.75}}{1.5 \cdot 10^{13} \text{ N}^{3.75}/\text{mm}^{7.5}} = 1.4 \cdot 10^{-4} \tag{54}$$

This value represents the contribution to the fatigue damage of the considered combination $117 \text{ N}/\text{m}^2 \leq \bar{q}_{10} < 123 \text{ N}/\text{m}^2$ and $490 \text{ N}/\text{m}^2 \leq \Delta \hat{q}_{10} < 560 \text{ N}/\text{m}^2$ and for the fully opened condition of the bridge. The procedure has to be repeated for each cell of the Markov matrix, and for each opening angle α. The fatigue damage of the wind fluctuations due to all combinations of $\bar{q}_{10}$, $\Delta \hat{q}_{10}$ and α is obtained by the summation of the damage for each individual cell of the Markov matrix and for each opening angle α (Eq. 37). The fatigue damage of the wind fluctuations is equal to $D_{w,tot} = 0.58$.

Next step is the evaluation of stress cycles Δs_1 and Δs_2. The contribution of the wind load to these stress cycles is determined with Eq. (38). The corresponding number of cycles is equal to the number of openings during the life of the bridge. The contribution to the fatigue damage of cyles Δs_1 and Δs_2 can be determined with a similar procedure as described above, leading to: $D_{\Delta s1} = 0.13$ and $D_{\Delta s2} = 0.01$, respectively. Thus, the total fatigue damage in the part considered is equal to: $D_{tot} = 0.58 + 0.13 + 0.01 = 0.72$. This is smaller than 1.0. Provided that the cylinder is not subjected to other fluctuating loads, such as traffic loads, the cylinder satisfies the requirements with respect to fatigue.

Eq. (1) represents the fatigue check in NEN 6786. The elaboration of that check is not provided here, only the result is provided: the fatigue unity check is equal to 1.0. Hence the cylinder also satisfies this fatigue check, but in this calculation there is no reserve.

The same calculation as provided above has been carried out for a variety of cases, with different values for the variables n_{op}, $\bar{v}_{10,\max}$, l, s_{weight} and s_{pre}, and for different S-N curves characterised by f_t and $f_{fat,re}$. In all cases considered, an opening consists of 2 minutes during which the bridge is being opened, 3 minutes during which the bridge is completely open, and 2 minutes during which the bridge is closed. For each case, the fatigue checks according to the procedure in NEN 6786 and according to the procedure in this paper have been determined for different values of the ratio between the stress and the wind pressure, C. Following, the value of C is selected that results in the fatigue unity check of NEN 6786 being equal to 1.0, and the value of C is selected that results in the fatigue damage of the procedure in this paper being equal to 1.0. The ratio between these two values of C is determined

$$\chi = \frac{C \text{ for which u.c.}_{\text{NEN6786}} = 1}{C \text{ for which } D_{\text{method in this paper}} = 1} \tag{55}$$

Hence, the ratio χ provides the difference between the two methods, expressed as stress ratio. The results of these calculations are provided in Table 10.

Table 10: Ratio χ for non-rotating parts

	n_{op} [-]	$5 \cdot 10^5$	$5 \cdot 10^5$	$5 \cdot 10^5$	$5 \cdot 10^5$	$5 \cdot 10^5$	$5 \cdot 10^5$	$5 \cdot 10^5$	$1 \cdot 10^4$
	$v_{10,max}$ [m/s]	14	14	14	14	14	22.5	10.7	14
	l [m]	20	80	20	20	20	20	20	20
	s_{weight} [MPa]	15	15	0	50	15	15	15	15
	s_{pre} [MPa]	-40	-40	-40	-40	0	-40	-40	-40
$f_t = 490$ [MPa] $f_{fat,re} = 50$ [MPa]		0.82	0.80	0.91	*)	0.98	0.58	1.20	0.57
$f_t = 900$ [MPa] $f_{fat,re} = 100$ [MPa]		1.03	0.98	1.03	0.93	1.03	0.46	*)	0.82
$f_t = 700$ [MPa] $f_{fat,re} = 50$ [MPa]		0.78	0.74	0.85	*)	0.94	0.55	1.09	0.41

*) factor could not be determined because static strength is decisive for the design

For the cases with $n_{op} = 5 \cdot 10^5$ and $\bar{v}_{10,max} = 14$ m/s, the ratio χ varies between 0.74 and 1.03, indicating that the method in this paper allows in general for an approximately equal or larger value of C – i.e. approximately equal or larger stress cycles – than the method in NEN 6786. The differences between the methods are larger in cases with a high value of $\bar{v}_{10,max} = 22.5$ m/s or a low value of $\bar{v}_{10,max} = 10.7$ m/s. This is due to the fact that the load for the fatigue check in NEN 6786 is directly related to the ultimate limit state load via Eq. (1), and this ultimate limit state load is directly related to $\bar{v}_{10,max}$, but the number of occurrences of the maximum wind velocity $\bar{v}_{10,max}$ is not considered in the fatigue check in NEN 6786. In reality, however, the probability of occurrence of a high value of $\bar{v}_{10}$ is smaller than that of a low value. In other words, the fatigue wind load spectrum is largely independent of $\bar{v}_{10,max}$. This aspect is not considered in the method in NEN 6786, but it is considered in the method in this paper.

Finally, the method in this paper allows for a larger value of C – i..e. larger stress cycles – for $n_{op} = 1 \cdot 10^4$. This is due to the fact that the factor ψ_{fat} in Eq. (1) is derived for $5 \cdot 10^5$ openings, and the actual number of openings is not considered in the method in NEN 6786. This number of openings is considered in the method in this paper.

6.2 Example of a rotating part

Similar to the example in Section 6.1, the fatigue damage can be determined for a rotating part. Consider the tooth of a gear. During full opening, the decisive tooth is fixed and continuously loaded and the stress cycles on the tooth are evaluated in the same way as for the non-rotating part in Section 6.1. When the bridge is being opened or closed, the fatigue damage is evaluated with Eq. (39) to (44), which again have to be evaluated for each cell of the Markov matrix and for each opening angle. Table 11 gives the ratio χ according to Eq. (55) for a number of cases with rotating parts.

Table 11: Ratio χ for rotating parts

	n_{op} [-]	$5\cdot10^5$	$5\cdot10^5$	$5\cdot10^5$	$5\cdot10^5$	$5\cdot10^5$	$5\cdot10^5$	$5\cdot10^5$	$5\cdot10^5$	$5\cdot10^5$	$1\cdot10^4$
	$v_{10,max}$ [m/s]	14	14	14	14	14	14	14	22.5	10.7	14
	l [m]	20	80	20	20	20	20	20	20	20	20
	s_{weight} [MPa]	15	15	0	15	15	15	15	15	15	15
	s_{pre} [MPa]	-40	-40	-40	0	0	-40	-40	-40	-40	-40
	f_ω [Hz]	15	15	15	15	15	4.99	100	15	15	15
f_t = 490 [MPa]	$f_{fat,re}$ = 100 [MPa]	0.97	0.97	0.99	0.97	0.97	1.09	0.81	0.46	1.62	0.97
f_t = 900 [MPa]	$f_{fat,re}$ = 100 [MPa]	0.77	0.79	0.83	0.77	0.77	0.78	0.75	0.40	1.05	0.53

The results for rotating parts in Table 11 are similar to those for non-rotating parts in Table 10: The differences between the methods are relatively small for the cases with $n_{op} = 5\cdot10^5$ and $\overline{v}_{10,max} = 14$ m/s. Large differences are determined for the cases with a high or low value for $\overline{v}_{10,max}$ and for a small number of openings.

7   Conclusions and recommendations

This paper presents a wind load model that can be used for fatigue design verifications of the operating mechanism of bascule bridges. The paper shows that it is possible to derive such a wind model with the basic principles behind EN 1991-1-4. The model consists of a Markov matrix with the probability of each combination of the mean wind load and wind fluctuation. By multiplying this probability with the total number of wind cycles during the life of the bridge, one obtains the fatigue load spectrum. The model requires more work and skills from the engineer than the current simple design check, but it is applicable to a wider range of bridges because it explicitly accounts for the number of openings, the average time of an opening and for the fact that the fatigue wind load spectrum is largely independent of $\overline{v}_{10,max}$. The new model will be applied in the standard NEN 6786 as an alternative for the simple design check.

Combination of the wind load model with other types of loads acting simultaneously on the bridge deck is considered in an approximate way. It is recommended to derive a more accurate method to account for the combinations of loads. In particular, effort is required to generate an accurate model for the load fluctuations generated by the dynamics of the system.

The model contains various conservatisms. In particular, the representation of the wind fluctuations with a narrow banded Gaussian process around f_c, the selection of the maximum wind shape factors for all wind directions, and the use of a fixed value for the central frequency, are conservative. It is recommended to quantify the effect of these conservatisms and to determine the value of the partial factor for the target reliability in a follow-up research.

References

EN 1991-1-4:2005 Eurocode 1: Actions on structures – Part 1-4: General actions – Wind actions

NEN 6786:2001 Voorschriften voor het ontwerpen van beweegbare bruggen (rules for the design of rotating bridges. In Dutch) (VOBB)

ISO 6336-3:2006 Calculation of load capacity of spur and helical gears – Part 3: Calculation of tooth bending strength

Holmes, J.D., *Wind Loading of Structures*, Taylor and Francis, 2001

Miner, M. A., 1945, Cumulative Damage in Fatigue, *Journal of Applied Mechanics*, Vol. 12, pp. 159-164, 1945

Palmgren, A.G., Die Lebensdauer von Kugellagern (Life Length of Roller Bearings. In German). *Zeitschrift des Vereines Deutscher Ingenieure* (VDI Zeitschrift), ISSN 0341-7258, Vol 68, No 14, pp. 339–341, 1924

Van Staalduinen, P.C. Achtergronden van de windbelasting volgens concept NEN6702 (Background of wind loads according to the draft of NEN6702. In Dutch) , *TNO-IBBC* report B-89-452, Rijswijk, 1989

Stroosma, D. *Dynamica van beweegbare bruggen, deel I: het aandrijfmechanisme* (Dynamics of rotating bridges, part I: rotating mechanism. In Dutch), RWS directie bruggen, 1980

Vrouwenvelder, A.C.W.M., Waarts, P.H., Van Staalduinen, P.C. Windbelasting op beweegbare bruggen (Wind loads on rotating bridges. In Dutch), *TNO-Bouw* report B-90-342, Rijswijk, 1990

Waarts, P.H., Van Staalduinen, P.C. Meting van de demping van een zestal beweegbare bruggen (Measurements of damping of 6 bridges. In Dutch), *TNO-Bouw* report B-90-326, Rijswijk, 1990

Wirsching, P.H., and Light, M.C. Fatigue under wide band random stresses, *Journal of the Structural Division* A.S.C.E. 106: pp. 1593-1607, 1980